Synthesis, structures, and catalytic activity in the Knoevenagel condensation reaction of three Co(Ⅱ), Cu(Ⅱ), and Cd(Ⅱ) coordination polymers based on an ether-bridged tetracarboxylic acid (English)

MU Jia-Xue, LI Xiong, ZOU Xun-Zhong, FENG An-Sheng, LI Yu

DOI:10.11862/CJIC.2023.024
Chinese J. Inorg. Chem., **2023**,**39**(00):-

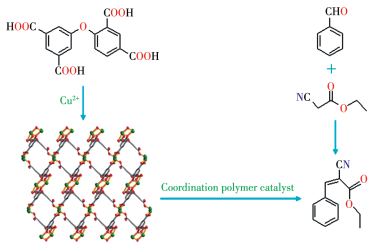

Three coordination polymers, 1D $[Co_2(\mu_4\text{-dia})(phen)_2(H_2O)_2]_n$ (**1**), 3D $[Cu_2(\mu_6\text{-dia})(bipy)_2]_n$ (**2**), and $\{[Cd_2(\mu_5\text{-dia})(\mu\text{-bpa})_2(H_2O)]\cdot H_2O\}_n$ (**3**), have been constructed and the structures and catalytic properties of the compounds were investigated.

基于醚氧桥联四羧酸配体构筑的三个钴(Ⅱ)、铜(Ⅱ)和镉(Ⅱ)配位聚合物的合成、结构和在Knoevenagel缩合反应中的催化性质

牟佳雪# 李 雄# 邹训重 冯安生 黎 彧*
(广东轻工职业技术学院,广东省特种建筑材料及其绿色制备工程技术研究中心,广州 510300)

摘要: 采用水热方法,选用醚氧桥联四羧酸配体H_4dia与菲咯啉(phen)、2,2′-联吡啶(bipy)或双(4-吡啶基)胺(bpa)分别与$CoCl_2\cdot 6H_2O$、$CuCl_2\cdot 2H_2O$和$CdCl_2\cdot 4H_2O$在160 ℃下反应,得到了一个一维链结构$[Co_2(\mu_4\text{-dia})(phen)_2(H_2O)_2]_n$ (**1**)和2个三维网络结构的配位聚合物$[Cu_2(\mu_6\text{-dia})(bipy)_2]_n$ (**2**)和$\{[Cd_2(\mu_5\text{-dia})(\mu\text{-bpa})_2(H_2O)]\cdot H_2O\}_n$ (**3**),并对其结构和催化性质进行了研究。研究表明,在50 ℃下配合物**2**在Knoevenagel缩合反应中显示出很好的催化活性。

关键词: 配位聚合物; 四羧酸; 催化性质; Knoevenagel缩合反应
中图分类号: O614.81+2; O614.121; O614.24+2 **文献标识码:** A **文章编号:** 1001-4861(2023)00-0000-09
DOI: 10.11862/CJIC.2023.024

Synthesis, structures, and catalytic activity in the Knoevenagel condensation reaction of three Co(Ⅱ), Cu(Ⅱ), and Cd(Ⅱ) coordination polymers based on an ether-bridged tetracarboxylic acid

MU Jia-Xue# LI Xiong# ZOU Xun-Zhong FENG An-Sheng LI Yu*
(*Guangdong Research Center for Special Building Materials and Its Green Preparation Technology, Guangdong Industry Polytechnic, Guangzhou* 510300, *China*)

Abstract: Three cobalt(Ⅱ), copper(Ⅱ), and cadmium(Ⅱ) coordination polymers, namely $[Co_2(\mu_4\text{-dia})(phen)_2(H_2O)_2]_n$ (**1**), $[Cu_2(\mu_6\text{-dia})(bipy)_2]_n$ (**2**), and $\{[Cd_2(\mu_5\text{-dia})(\mu\text{-bpa})_2(H_2O)]\cdot H_2O\}_n$ (**3**) have been constructed hydrothermally using H_4dia (5-(2,5-dicarboxyphenoxy)isophthalic acid), phen (phen=1,10-phenanthroline), bipy (2,2′-bipyridine), bpa (bis(4-pyridyl)amine), and cobalt, copper and cadmium chlorides at 160 ℃. The products were isolated as stable crystalline solids and were characterized by IR spectra, elemental analyses, thermogravimetric analyses, and single-crystal X-ray diffraction analyses. Single-crystal X-ray diffraction analyses reveal that three compounds crystallize in the monoclinic or triclinic systems, space groups $P2_1/n$, $P2_1/c$, or $P\bar{1}$. Compound **1** discloses a 1D double-chain structure. Compounds **2** and **3** show 3D frameworks. The catalytic activity in the Knoevenagel condensation reaction of these compounds was investigated. Compound **2** exhibited excellent catalytic activity in the Knoevenagel condensation reaction at 50 ℃. CCDC: 2209559, **1**; 2209560, **2**; 2209561, **3**.

Keywords: coordination polymer; tetracarboxylic acid; catalytic properties; Knoevenagel condensation reaction

收稿日期:2022-09-30。收修改稿日期:2022-12-14。
广东省教育厅青年人才项目(No.2022KQNCX174)资助。
#共同第一作者。
*通信联系人。E-mail:liyuletter@163.com

0 Introduction

As one of the most promising crystalline materials, metal-organic architectures have attracted tremendous attention in the past few decades because of their diversities[1-3], and display extensive potential applications in gas adsorption/separation[4-5], sensing[6-7], heterogeneous catalysis[8-12], bioactivity[13-14], and so on[15-16].

The synthesis of coordination polymers (CPs) can be adjusted for generating specific structures and topologies with property-driven applications[17-19]. Despite considerable progress made in this area, it is often challenging to predict the structures of CPs during the self-assembly generation, since a variety of factors can affect their crystallization. Such factors may include structural features of organic linkers and supporting ligands[20-22], coordination behavior of metal ions[23-24], type of solvent[25-26], reaction temperature[27-28], and pH value[29-30].

Aromatic multi-carboxylic acids represent the most important class of organic linkers for CPs, owing to their versatile coordination chemistry, good thermal stability, adjustable level of deprotonation, and ability to participate in different noncovalent interactions[9,11-12,24]. Recently, our groups have been focused on designing functional CPs based on multi-carboxylate biphenyl or triphenyl blocks, which feature a diversity of coordination modes toward different metal(Ⅱ) centers[9,31-32]. As a further continuation of this research line, we have selected in the present study a little explored ether-bridged tetracarboxylate ligand, 5-(2,5-dicarboxyphenoxy)isophthalic acid (H_4dia), and tested it as an adaptable linker for constructing new metal-organic architectures by hydrothermal synthesis.

Herein, we report the synthesis, crystal structures, and catalysis of three Co(Ⅱ), Cu(Ⅱ), and Cd(Ⅱ) CPs with H_4dia and phen (1,10-phenanthroline)/bipy (2,2′-bipyridine)/bpa (bis(4-pyridyl)amine).

1 Experimental

1.1 Reagents and physical measurements

All chemicals and solvents were obtained from commercial suppliers. H_4dia was acquired from Jinan Henghua Sci. & Tec. Co., Ltd. Carbon, hydrogen, and nitrogen of the compounds were determined using an Elementar Vario EL elemental analyzer. IR spectrum was recorded using KBr pellets and a Bruker EQUINOX 55 spectrometer. Thermogravimetric analysis (TGA) data were collected on a LINSEIS STA PT1600 thermal analyzer with a heating rate of 10 ℃·min^{-1}. Powder X-ray diffraction (PXRD) patterns were measured on a Rigaku-Dmax 2400 diffractometer using Cu $K\alpha$ radiation (λ=0.154 06 nm); the X-ray tube was operated at 40 kV and 40 mA; the data collection range was between 5° and 45°. Solution ^{1}H NMR spectra were recorded on a JNM ECS 400M spectrometer.

1.2 Synthesis of $[Co_2(\mu_4\text{-dia})(phen)_2(H_2O)_2]_n$ (1)

A mixture of $CoCl_2\cdot 6H_2O$ (0.048 g, 0.2 mmol), H_4dia (0.035 g, 0.1 mmol), phen (0.040 g, 0.2 mmol), NaOH (0.016 g, 0.4 mmol), and H_2O (10 mL) was stirred at room temperature for 15 min, and then sealed in a 25 mL Teflon-lined stainless steel vessel, and heated at 120 ℃ for 3 d, followed by cooling to room temperature at a rate of 10 ℃·h^{-1}. Pink block-shaped crystals were isolated manually, and washed with distilled water. Yield: 45% (based on H_4dia). Anal. Calcd. for $C_{40}H_{26}Co_2N_4O_{11}$(%): C 56.09, H 3.06, N 6.54; Found (%): C 55.83, H 3.08, N 6.51. IR (KBr, cm^{-1}): 3 622w, 3 297w, 3 067w, 1 615m, 1 588m, 1 543m, 1 519w, 1 458w, 1 426s, 1 382s, 1 342s, 1 310w, 1 225w, 1 201w, 1 128w, 1 080w, 967w, 919w, 871w, 850m, 803w, 778w, 727m, 698w, 642w.

1.3 Synthesis of $[Cu_2(\mu_6\text{-dia})(bipy)_2]_n$ (2)

A mixture of $CuCl_2\cdot 2H_2O$ (0.034 g, 0.2 mmol), H_4dia (0.035 g, 0.10 mmol), bipy (0.031 g, 0.20 mmol), NaOH (0.016 g, 0.40 mmol), and H_2O (10 mL) was stirred at room temperature for 15 min, then sealed in a 25 mL Teflon-lined stainless steel vessel, and heated at 120 ℃ for 3 d, followed by cooling to room temperature at a rate of 10 ℃·h^{-1}. Blue block-shaped crystals were isolated manually, washed with distilled water, and dried. Yield: 43% (based on H_4dia). Anal. Calcd. for $C_{36}H_{22}Cu_2N_4O_9$(%): C 55.32, H 2.84, N 7.17; Found(%): C 55.54, H 2.82, N 7.21. IR (KBr, cm^{-1}): 1 638s, 1 615s, 1 543s, 1 579m, 1 475w, 1 442w, 1 357s, 1 285w, 1 249w, 1 209w, 1 161w, 1 125w, 1 080w, 1 060w, 1 027w, 967w, 923w, 899w, 859w, 771m, 730w, 678w, 649w.

1.4 Synthesis of $\{[Cd_2(\mu_5\text{-dia})(\mu\text{-bpa})_2(H_2O)]\cdot H_2O\}_n$ (3)

A mixture of $CdCl_2\cdot H_2O$ (0.040 g, 0.2 mmol), H_4dia (0.035 g, 0.1 mmol), bpa (0.034 g, 0.2 mmol), NaOH (0.016 g, 0.4 mmol), and H_2O (10 mL) was stirred at room temperature for 15 min, and then sealed in a 25 mL Teflon-lined stainless steel vessel, and heated at 120 ℃ for 3 d, followed by cooling to room temperature at a rate of 10 ℃·h^{-1}. Colourless block-shaped crystals were isolated manually and washed with distilled water. Yield: 47% (based on H_4dia). Anal. Calcd. for $C_{36}H_{28}Cd_2N_6O_{11}$(%): C 45.73, H 2.98, N 8.89; Found(%): C 45.85, H 3.00, N 8.86. IR (KBr, cm^{-1}): 3 631w, 3 259, 3 164w, 3 064w, 1 613s, 1 593s, 1 540s, 1 521s, 1 480w, 1 445w, 1 425w, 1 373s, 1 341w, 1 249w, 1 209m, 1 141w, 1 081w, 1 014m, 977w, 921w, 902w, 861w, 845w, 814w, 786w, 734w, 693w, 641w.

The compounds are insoluble in water and common organic solvents, such as methanol, ethanol, acetone, and DMF.

1.5 Structure determination

Three single crystals with dimensions of 0.23 mm×0.20 mm×0.18 mm (**1**), 0.21 mm×0.20 mm×0.18 mm (**2**), and 0.20 mm×0.19 mm×0.15 mm (**3**) were collected at 293(2) K on a Bruker SMART APEX Ⅱ CCD diffractometer with Cu $K\alpha$ (λ=0.154 178 nm). The structures were solved by direct methods and refined by full-matrix least-square on F^2 using the SHELXTL-2014 program. All non-hydrogen atoms were refined anisotropically. All the hydrogen atoms (except for the ones bound to water molecules) were placed in calculated positions with fixed isotropic thermal parameters included in structure factor calculations in the final stage of full-matrix least-squares refinement. The hydrogen atoms of water molecules were located by different maps and constrained to ride on their parent O atoms. For **1**, the O_{ether} atom of the dia^{2-} ligand was split over two sites with refined occupancies of 0.55 and 0.45. Two benzene rings of the ligand were also split over two sites with refined occupancies of 0.55 and 0.45, 050 and 0.50, respectively. A summary of the crystallography data and structure refinements for **1**-**3** is given in Table S1 (Supporting information). The selected bond lengths and angles for compounds **1**-**3** are listed in Table S2. Hydrogen bond parameters of compounds **1** and **3** are given in Table S3 and S4.

CCDC: 2209559, **1**; 2209560, **2**; 2209561, **3**.

1.6 Catalysis of the Knoevenagel condensation reaction of aldehydes

In a typical test, a suspension of aromatic aldehyde (0.50 mmol, benzaldehyde as a model substrate), ethyl cyanoacetate (1.0 mmol), and catalyst (typically x=2%) in methanol (1.0 mL) was stirred at 50 ℃. After the desired reaction time, the catalyst was removed by centrifugation, followed by evaporation of the solvent from the filtrate under reduced pressure to give a crude solid. This was dissolved in $CDCl_3$ and analyzed by ^{1}H NMR spectroscopy for the quantification of products (Fig.S1). To perform the recycling experiment, the catalyst was isolated by centrifugation, washed with methanol, dried at room temperature, and reused. The subsequent steps were performed as described above.

2 Results and discussion

2.1 Description of the structure

2.1.1 Structure of compound **1**

This compound is a 1D CP and its asymmetric unit encloses two Co(Ⅱ) centers (Co1 and Co2), one μ_4-dia^{4-} block, two phen moieties, and two H_2O molecules (Fig.1). Both Co centers are six-coordinated and assume a distorted octahedral $\{CoN_2O_4\}$ geometry, which is

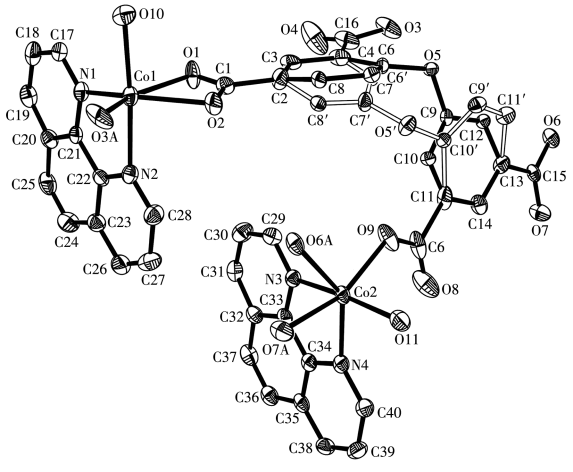

H atoms are omitted for clarity; Symmetry code: A: $x-1$, y, z

Fig.1 Drawing of the asymmetric unit of compound **1** with a 30% probability of thermal ellipsoids

occupied by three carboxylate oxygen atoms from two μ_4-dia^{4-} ions, one H_2O molecule as well as two N atoms from the phen moiety. The Co—O (0.198 1(5)-0.224 7(4) nm) and Co—N (0.209 0(6)-0.214 1(6) mn) bonds show typical distances[12,24,31]. The dia^{4-} block functions as a μ_4-bridging ligand with four COO^- groups being monodentate or bidentate (mode Ⅰ, Scheme 1). In the μ_4-dia^{4-}, two aromatic rings reveal a dihedral angle of 75.94° and a C—O_{ether}—C angle of 114.79°. These carboxylate functionalities unite the Co(Ⅱ) centers to form a 1D double chain (Fig.2).

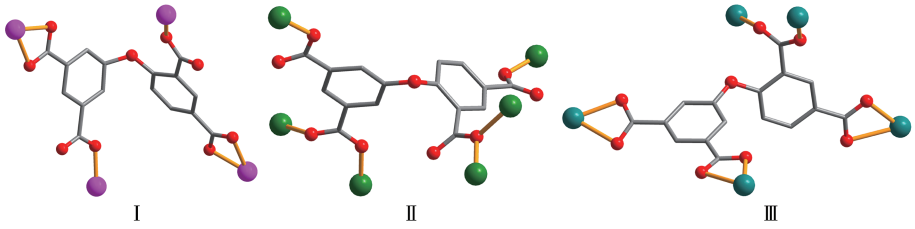

Scheme 1 Coordination modes of the dia^{4-} ligands in compounds **1-3**

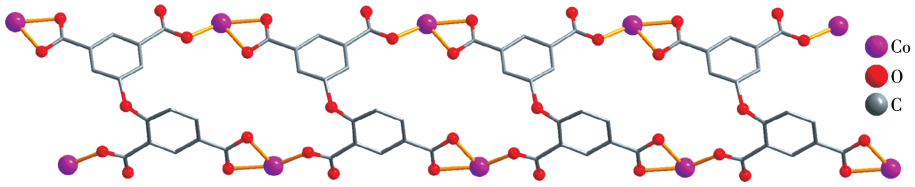

phen and H_2O ligands are omitted for clarity

Fig.2 A perspective of 1D double chain along the *b*-axis

2.1.2 Structure of compound **2**

CP **2** shows a 3D framework structure. The asymmetric unit contains two Cu centers (Cu1 and Cu2), a μ_6-dia^{4-} linker, and two bipy moieties. As shown in Fig. 3, both Cu1 and Cu2 centers are five-coordinate and feature a distorted square pyramidal $\{CuN_2O_3\}$ environment with the τ parameter of 0.113 or 0.078 (τ= 0 or 1 for a regular square pyramidal or trigonal-bipyramidal geometry, respectively)[33]. The Cu1 and Cu2 centers are surrounded by three carboxylate O atoms from three μ_6-dia^{4-} spacers and two N atoms from the bipy moiety. The Cu—O (0.193 2(5)-0.235 3(4) nm) and Cu—N (0.199 7(5)-0.203 5(5) nm) bonds are within standard values[11,31]. The dia^{4-} ligand takes a μ_6-coordination fashion with COO^- groups being monodentate or bidentate (mode Ⅱ, Scheme 1). The μ_6-dia^{4-} moiety displays the dihedral angles between the aromatic rings of 81.06° and the C—O_{ether}—C angle of 115.54°. Two crystallographically Cu1 and Cu2 ions are bridged through two carboxylate groups or two carboxylate O atoms from two different dia^{4-} blocks, respectively, giving rise to two Cu_2 subunits (Fig.4). These Cu_2 subunits are multiply interlinked by the remaining carboxylate groups of the dia^{4-} blocks to form a 3D metal-organic framework (Fig.5)

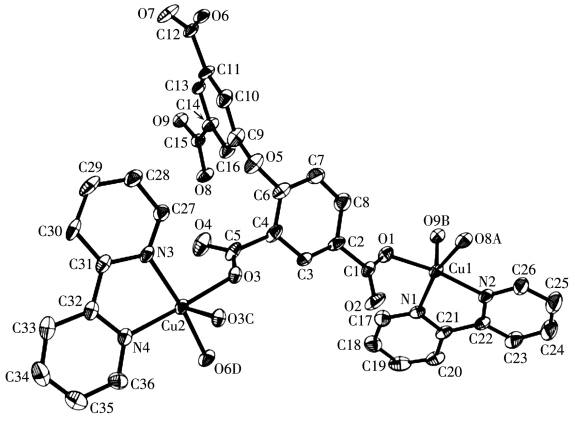

H atoms are omitted for clarity; Symmetry codes: A: *x*+1, *y*, *z*; B: −*x*+1, −*y*, −*z*+1; C: −*x*+1, −*y*+1, −*z*; D: *x*, *y*+1, *z*

Fig.3 Drawing of the asymmetric unit of compound **2** with a 30% probability of thermal ellipsoids

2.1.3 Structure of compound **3**

This compound also has a 3D metal-organic framework. The asymmetric unit contains two Cd (Ⅱ) centers (Cd1 and Cd2), a μ_5-dia^{4-} block, two μ-bpa

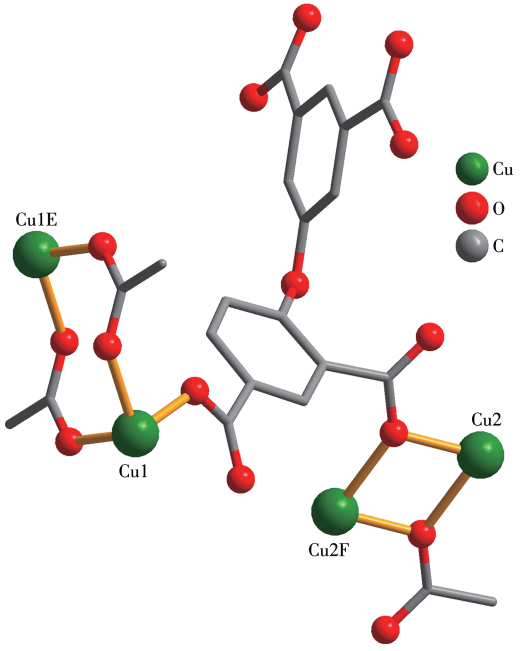

Symmetry codes: E: −*x*+2, −*y*, −*z*+1; F: −*x*+1, −*y*+1, −*z*

Fig.4　Two Cu_2 units of compound **2**

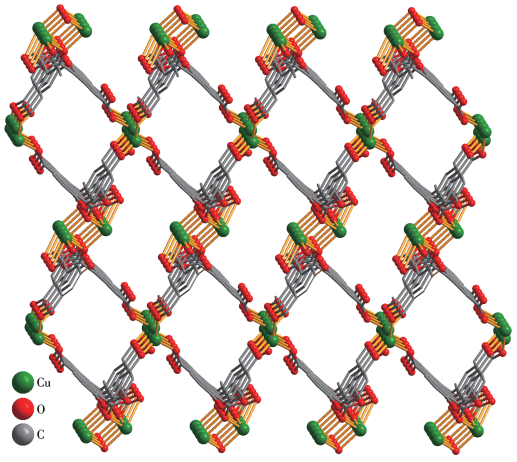

Symmetry codes: E: −*x*+2, −*y*, −*z*+1; F: −*x*+1, −*y*+1, −*z*

Fig.5　Three-dimensional metal-organic framework viewed along the *b*-axis

moieties, an H_2O ligand, and a lattice water molecule. The Cd1 center is seven-coordinate and assumes a distorted pentagonal bipyramidal $\{CdN_2O_5\}$ environment, which is populated by four carboxylate O atoms from two μ_5-dia^{4-} blocks, one H_2O ligand, and two N donors of two different μ-bpa moieties (Fig.6). The Cd2 center is six-coordinate and features a distorted octahedral $\{CdN_2O_4\}$ geometry, which is occupied by four carboxylate oxygen atoms from three μ_5-dia^{4-} ligands as well as two N atoms from two different μ-bpa moieties. The Cd—O (0.226 4(3)-0.249 1(4) nm) and Cd—N (0.228 1(4)-0.238 8(4) nm) bonds show typical distances[24,31-32]. The dia^{4-} block acts as a μ_5-spacer (mode Ⅲ, Scheme 1), in which four COO^- groups are μ-bridging bidentate or bidentate. In the μ_5-$deta^{4-}$, two aromatic rings reveal a dihedral angle of 75.00° and a C—O_{ether}—C angle of 116.11°. The adjacent Cd(Ⅱ) atoms are connected via μ_5-dia^{4-} blocks and μ-bpa moieties to form a 3D metal-organic framework (Fig.7).

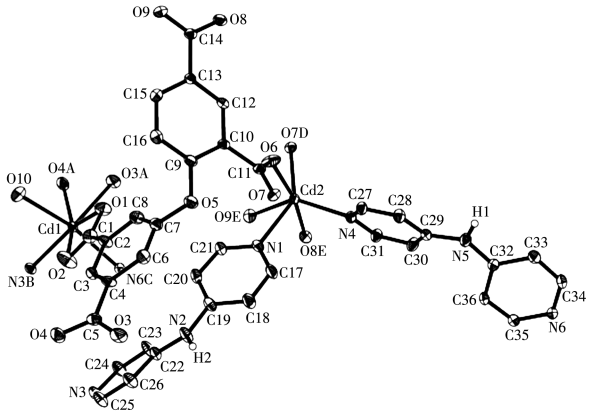

H atoms are omitted for clarity except for NH groups; Symmetry codes: A: *x*, *y*−1, *z*; B: −*x*, *y*−1/2, −*z*+1/2; C: −*x*+1, −*y*+1, −*z*+1; D: −*x*+1, *y*−1/2, −*z*+1/2; E: *x*, −*y*+1/2, *z*+1/2

Fig.6　Drawing of the asymmetric unit of compound **3** with a 30% probability of thermal ellipsoids

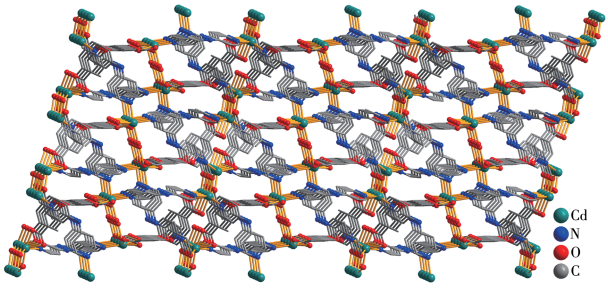

Water molecules are omitted for clarity

Fig.7　Three-dimensional metal-organic framework viewed along the *a*-axis and *c*-axis

2.2　TGA analysis

To determine the thermal stability of CPs **1**-**3**, their thermal behaviors were investigated under a nitrogen atmosphere by TGA. As shown in Fig.8, compound **1** lost its two coordinated H_2O molecules in a range of 168-214 ℃ (Obsd. 4.4%, Calcd. 4.2%), followed by the decomposition at 314 ℃. Compound **2** does not contain H_2O and solvent molecules and its framework main-

tained stability up to 271 ℃. For 3D CP **3**, the TGA curve displayed a loss of one lattice and one coordinated water molecule between 54 and 162 ℃ (Obsd. 3.6%, Calcd. 3.8%), whereas a dehydrated solid was then stable up to 346 ℃.

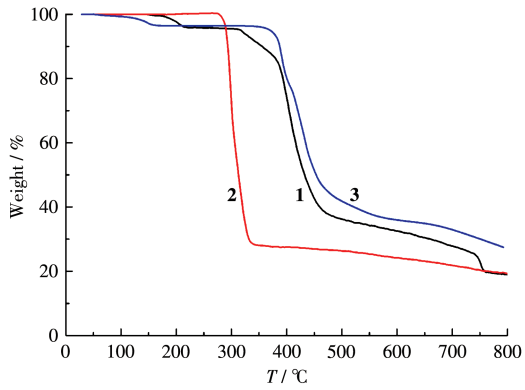

Fig.8 TGA curves of compounds **1**-**3**

2.3 Catalysis of the Knoevenagel condensation reaction

Considering the potential of different metal (Ⅱ) coordination compounds to act as catalysts in the Knoevenagel condensation[9,34-36], we probed compounds **1**-**3** as heterogeneous catalysts in this reaction using assorted aldehydes with ethyl cyanoacetate. As a model substrate, benzaldehyde was treated with ethyl cyanoacetate at 50 ℃ in a methanol medium to form a 2-cyano-3-phenyl-2-propenoic acid ethyl ester product (Scheme 2, Table 1). The influence of different reaction parameters (*i. e.*, reaction time, temperature, solvent type, catalyst loading and recycling, and substrate scope) was studied.

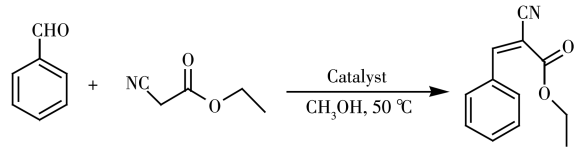

Scheme 2 Cu-catalyzed the Knoevenagel condensation reaction of benzaldehyde with ethyl cyanoacetate

Compound **2** revealed the highest activity, resulting in a quantitative conversion of benzaldehyde to 2-cyano-3-phenyl-2-propenoic acid ethyl ester (Table 1 and Fig. S1). Compound **2** was used to research the influence of different reaction parameters. The yield was accumulated with a yield increase from 53% to 100% on prolonging the reaction from 1 to 4 h (Table 1, Entry 1-4). The influence of catalyst amount was also investigated, revealing a product yield growth from 96% to 100% on increasing the loading of the catalyst (molar fraction) from 1% to 2% (Entry 4 and 5). Entry 6 showed that 2% compound **2** catalyzed the reaction and produced the product in 93% at 40 ℃; however, a

Table 1 Cu-catalyzed Knoevenagel condensation reaction of benzaldehyde with ethyl cyanoacetate

Entry	Catalyst	Time / h	Temperature / ℃	Catalyst loading / %	Solvent	Yield* / %
1	**2**	1	50	2.0	CH_3OH	53
2	**2**	2	50	2.0	CH_3OH	77
3	**2**	3	50	2.0	CH_3OH	90
4	**2**	4	50	2.0	CH_3OH	100
5	**2**	4	50	1.0	CH_3OH	96
6	**2**	4	40	2.0	CH_3OH	93
7	**2**	4	50	2.0	H_2O	57
8	**2**	4	50	2.0	C_2H_5OH	55
9	**2**	4	50	2.0	CH_3CN	37
10	**2**	4	50	2.0	$CHCl_3$	32
11	**1**	4	50	2.0	CH_3OH	81
12	**3**	4	50	2.0	CH_3OH	74
13	Blank	4	50	—	CH_3OH	2
14	$CuCl_2$	4	50	2.0	CH_3OH	13
15	H_4dia	4	50	2.0	CH_3OH	15

* Calculated by ^{1}H NMR spectroscopy: $n_{product}/n_{aldehyde}\times100\%$.

mildly elevated temperature of 50 ℃ led to nearly quantitative. In addition to methanol, other solvents were tested. Water, ethanol, acetonitrile, and chloroform were less suitable (Yield: 32%-57%).

In comparison with **2**, compounds **1** and **3** were less active, resulting in the maximum product yields in a range of 74%-81% (Entry 11 and 12, Table 1). It should be highlighted that under similar reaction conditions, the Knoevenagel condensation of benzaldehyde was significantly less efficient in the absence of the catalyst (Yield: 2%) or when using H_4dia (Yield: 15%) or $CuCl_2$ (Yield: 13%) as catalysts (Entry 13-15, Table 1). Although a connection between catalytic activity and the structural characteristic of the catalyst may not be fully established in the present work, the superior activity of compound **2** might be attributed to the existence of more easily accessible Lewis acid metal sites[35,37].

Different substituted benzaldehyde substrates were used to study the substrate scope in the Knoevenagel condensation with ethyl cyanoacetate. These tests were run under optimized conditions (2.0% of **2**, CH_3OH, 50 ℃, 4 h). The corresponding products were obtained in the yields varying from 36% to 100% (Table 2). Benzaldehydes containing a strong electron-withdrawing group (*e.g.*, nitro, and chloro substituent in the ring) revealed the best efficiency (Entry 2-5, Table 2), which can be explained by an increased electrophilicity of substrates. The benzaldehydes possessing an electron-donating functionality (*e.g.*, methyl or methoxy group) led to lower product yields (Entry 7 and 8, Table 2).

Table 2 Knoevenagel condensation reaction of various aldehydes with ethyl cyanoacetate catalyzed by compound 2[a]

Entry	Substituted benzaldehyde substrate (R—C_6H_4CHO)	Yield[b] / %
1	R=H	100
2	R=2-NO_2	100
3	R=3-NO_2	100
4	R=4-NO_2	100
5	R=4-Cl	83
6	R=4-OH	40
7	R=4-CH_3	65
8	R=4-OCH_3	36

[a] Reaction conditions: aldehyde (0.5 mmol), malononitrile (1.0 mmol), catalyst 2 (2.0%), and CH_3OH (1.0 mL) at 50 ℃; [b] Calculated by ^{1}H NMR spectroscopy.

Finally, the recyclability of catalyst **2** was tested. After each reaction cycle, the catalyst was separated via centrifugation, washed with CH_3OH, dried in air at *ca*. 25 ℃, and reused in the next cycle. The yields were 100%, 99%, 97%, and 96% for the second to the fifth run, respectively. The obtained results proved that compound **2** preserved the activity for at least five reaction cycles. Besides, the PXRD patterns (Fig. 9) confirm that the structure of **2** is maintained, despite the appearance of several additional signals or the widening of some peaks. These alterations might be expected after a few catalytic cycles and are explained by the presence of some impurities or a decrease in crystallinity. In terms of the observed activity, compound **2** generally appears to be superior in the Knoevenagel condensation of aldehydes if compared to several reported CPs (Table S5).

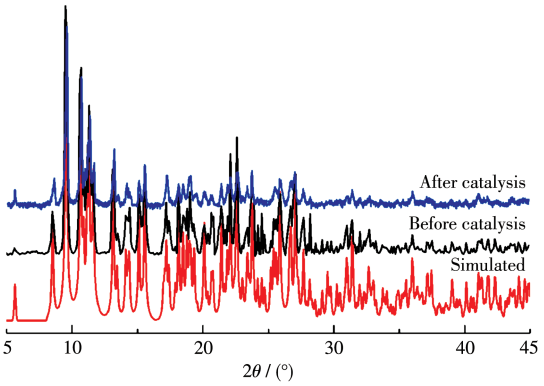

Fig.9 PXRD patterns for **2**

3 Conclusions

In summary, we have synthesized three Co(Ⅱ), Cu(Ⅱ), and Cd(Ⅱ) CPs (**1**-**3**) based on a tetracarboxylate ligand. Compounds **1**-**3** disclose a 1D double chain and 3D framework, respectively. The catalytic properties of these compounds were investigated. Compound **2** revealed excellent catalytic activity in the Knoevenagel condensation reaction at 50 ℃.

Supporting information is available at http://www.wjhxxb.cn

References:

[1]Lustig W P, Li J. Luminescent metal-organic frameworks and coordination polymers as alternative phosphors for energy efficient lighting devices. *Coord. Chem. Rev.*, **2018**,**373**(15):116-147

[2]Chakraborty G, Park I, Medishetty R, Vittal J J. Two-dimensional metal-organic framework materials: Synthesis, structures, properties and applications. *Chem. Rev.*, **2021**,**121**(7):3751-3891

[3]Easun T L, Moreau F, Yan Y, Yang S, Schroder M. Structural and dynamic studies of substrate binding in porous metal-organic frameworks. *Chem. Soc. Rev.*, **2017**,**46**(1):239-274

[4]Fan W D, Yuan S, Wang W J, Feng L, Liu X P, Zhang X R, Wang X, Kang Z X, Dai F N, Yuan D Q, Sun D F, Zhou H C. Optimizing multivariate metal-organic frameworks for efficient C_2H_2/CO_2 separation. *J. Am. Chem. Soc.*, **2020**,**142**(19):8728-8737

[5]Zheng B, Luo X, Wang Z, Zhang S, Yun R, Huang L, Zeng W, Liu W. An unprecedented water stable acylamide-functionalized metal-organic framework for highly efficient CH_4/CO_2 gas storage/separation and acid-base cooperative catalytic activity. *Inorg. Chem. Front.*, **2018**,**5**(9):2355-2363

[6]Patel N, Shukla P, Lama P, Das S, Pal T K. Engineering of metal-organic frameworks as ratiometric sensors. *Cryst. Growth Des.*, **2022**,**22**(5):3518-3564

[7]Li J, Tian J F, Yu H H, Fan M Y, Li X, Liu F B, Sun J, Su Z M. Controllable synthesis of metal-organic frameworks based on anthracene ligands for high-sensitivity fluorescence sensing of Fe^{3+}, $Cr_2O_7^{2-}$, and TNP. *Cryst. Growth Des.*, **2022**,**22**(5):2954-2963

[8]Zhao L, Du Z G, Ji G F, Wang Y F, Cai W, He C, Duan C Y. Eosin Y-containing metal-organic framework as a heterogeneous catalyst for direct photoactivation of inert C—H bonds. *Inorg. Chem.*, **2022**,**61**(19):7256-7265

[9]赵素琴, 顾金忠. 两个二苯醚四羧酸-钴(Ⅱ)配位聚合物的合成、结构和催化性质. 无机化学学报, **2022**,**38**(1):161-170
ZHAO S Q, GU J Z. Synthesis, structures and catalytic activity in Knoevenagel condensation reaction of two diphenyl ether tetracarboxylic acid-Co(Ⅱ) coordination polymers. *Chinese J. Inorg. Chem.*, **2022**,**38**(1):161-170

[10]Wei Y S, Zhang M, Zou R, Xu Q. Metal-organic framework-based catalysts with single metal sites. *Chem. Rev.*, **2020**,**120**(21):12089-12174

[11]Gu J Z, Wen M, Cai Y, Shi Z F, Arol A S, Kirillova M V, Kirillov A M. Metal-organic architectures assembled from multifunctional polycarboxylates: Hydrothermal self-assembly, structures, and catalytic activity in alkane oxidation. *Inorg. Chem.*, **2019**,**58**(4):2403-2412

[12]Gu J Z, Wen M, Cai Y, Shi Z F, Nesterov D S, Kirillova M V, Kirillov A M. Cobalt(Ⅱ) coordination polymers assembled from unexplored pyridine-carboxylic acids: Structural diversity and catalytic oxidation of alcohols. *Inorg. Chem.*, **2019**,**58**(9):5875-5885

[13]Zhu Y, Xin N, Qiao Z, Chen S, Zeng L, Zhang Y, Wei D, Sun J, Fan H. Bioactive MOFs based theranostic agent for highly effective combination of multimodal imaging and chemo-phototherapy. *Adv. Healthcare Mater.*, **2020**,**9**(14):2000205

[14]Feng J, Ren W X, Kong F, Dong Y B. Recent insight into functional crystalline porous frameworks for cancer photodynamic therapy. *Inorg. Chem. Front.*, **2021**,**8**(4):848-879

[15]Neumann T, Ceglarska M, Germann L S, Rams M, Dinnebier R E, Suckert S, Jess I, Naether C. Structures, thermodynamic relations, and magnetism of stable and metastable $Ni(NCS)_2$ coordination polymers. *Inorg. Chem.*, **2018**,**57**(6):3305-3314

[16]Makhanya N, Oboirien B, Ren J, Musyoka N, Sciacovelli A. Recent advances on thermal energy storage using metal-organic frameworks (MOFs). *J. Energy Storage*, **2021**,**34**:102179

[17]Huang W H, Zhang X X, Zhao Y N. Recent progress and perspectives on the structural design on metal-organic zeolite (MOZ) frameworks. *Dalton Trans.*, **2021**,**50**(1):15-28

[18]Raptopoulou C P. Metal-organic frameworks: Synthetic methods and potential applications. *Materials*, **2021**,**14**(2):310

[19]Zheng X D, Lu T B. Constructions of helical coordination compounds. *CrystEngComm*, **2010**,12(2):324-336

[20]Zhan G, Zhong W, Wei Z, Liu Z, Liu X. Roles of phenol groups and auxiliary ligand of copper(Ⅱ) complexes with tetradentate ligands in the aerobic oxidation of benzyl alcohol. *Dalton Trans.*, **2017**,**46**(25):8286-8297

[21]Fan G, Hong L, Zheng X, Zhou J, Zhan J, Chen Z, Liu S. Growth inhibition of microcystic aeruginosa by metal-organic frameworks: Effect of variety, metal ion and organic ligand. *RSC Adv.*, **2018**,**8**(61):35314-35326

[22]Lei Z, Hu L, Yu Z H, Yao Q Y, Chen X, Li H, Liu R M, Li C P, Zhu X D. Ancillary ligand enabled structural and fluorescence diversity in metal-organic frameworks: Application for the ultra-sensitive detection of nitrofuran antibiotics. *Inorg. Chem. Front.*, **2021**,**8**(5):1290-1296

[23]Yang Y, Lu C, Wang H, Liu X. Amide bond cleavage initiated by coordination with transition metal ions and tuned by an auxiliary ligand. *Dalton Trans.*, **2016**,**45**(25):10289-10296

[24]Gu J Z, Cui Y H, Liang X X, Wu J, Lv D Y, Kirillov A M. Structurally distinct metal-organic and H-bonded networks derived from 5-(6-carboxypyridin-3-yl)isophthalic acid: Coordination and template effect of 4,4′-bipyridine. *Cryst. Growth Des.*, **2016**,**16**(8):4658-4670

[25]Wei N, Zhang M Y, Zhang X N, Li G M, Zhang X D. Two series of solvent-dependent lanthanide coordination polymers demonstrating tunable luminescence and catalysis properties. *Cryst. Growth Des.*, **2014**,**14**(6):3002-3009

[26]Kühne I A, Carter A B, Kostakis G E, Anson C E, Powell A K. Varying the dimensionality of Cu(Ⅱ)-based coordination polymers through solvent influence. *Crystals*, **2020**,**10**(10):893

[27]Li Y, Wu J, Gu J Z, Qiu W D, Feng A S. Temperature-dependent syntheses of two manganese(Ⅱ) coordination compounds based on an ether-bridged tetracarbolylic acid. *Chin. J. Struct. Chem.*, **2020**,**39**(4):727-736

[28]邹训重, 吴疆, 顾金忠, 赵娜, 冯安生, 黎彧. 两个基于刚性线型三

羧酸配体的镍(Ⅱ)配合物的合成. 无机化学学报, **2019**,**35**(9):1705-1711

ZHOU X Z, WU J, GU J Z, ZHAO N, FENG A S, LI Y. Syntheses of two nickel(Ⅱ) coordination compounds based on a rigid linear tricarboxylic acid. *Chinese J. Inorg. Chem.*, **2019**,**35**(9):1705-1711

[29]Gu J Z, Gao Z Q, Tang Y. pH and auxiliary ligand influence on the structural variations of 5(2′-carboxylphenyl) nicotate coordination polymers. *Cryst. Gorwth Des.*, **2012**,**12**(6):3312-3323

[30]Zhong D C, Lu W G, Deng J H. Two three-dimensional cadmium(Ⅱ) coordination polymers based on 5-amino-tetrazolate and 1,2,4,5-benzenetetracarboxylate: The pH value controlled syntheses, crystal structures and luminescent properties. *CrystEngComm*, **2014**,**16**(21):4633-4640

[31]Cheng X Y, Guo L R, Wang H Y, Gu J Z, Yang Y, Kirillova M V, Kirillov A M. Coordination polymers from biphenyl-dicarboxylate linkers: Synthesis, structural diversity, interpenetration, and catalytic properties. *Inorg. Chem.*, **2022**,**61**(32):12577-12590

[32]Gu J Z, Wan S M, Dou W, Kirillova M V, Kirillov A M. Coordination polymers from unexplored biphenyl-tricarboxylate linker: Hydrothermal synthesis, structural traits and catalytic cyanosilylation. *Inorg. Chem. Front.*, **2021**,**8**(5):1229-1242

[33]Addison A W, Rao T N, Reedijk J, Van Rijin J, Verschoor G C. Synthesis, structure, and spectroscopic properties of copper(Ⅱ) compounds containing nitrogen sulfur donor ligands-the crystal and molecular-structure of aqua[1,7-bis(*N*-methylbenzimidazol-2′-yl)-2,6-dithiaheptane] copper(Ⅱ) perchlorate. *J. Chem. Soc. Dalton Trans.*, **1984**,**7**:1349-1356

[34]Chen H T, Fan L M, Hu T P, Zhang X T. 6*s*-3*d* {Ba_3Zn_4}-organic framework as an effective heterogeneous catalyst for chemical fixation of CO_2 and Knoevenagel condensation reaction. *Inorg. Chem.*, **2021**,**60**(5):3384-3392

[35]Karmakar A, Rúbio G M D M, Guedes da Silva M F C, Pombeiro A J L. Synthesis of metallomacrocycle and coordination polymers with pyridine-based amidocarboxylate ligands and their catalytic acitivities towards the Henry and Knoevenagel reaction. *ChemistryOpen*, **2018**,**7**(11):865-877

[36]Almáši M, Zeleňák V, Opanasenko M, Čejka J. A novel nickel metal-organic framework with fluorite-like structure: Gas adsorption properties and catalytic activity in Knoevenagel condensation. *Dalton Trans.*, **2014**,**43**(9):3730-3738

[37]Cheng X Y, Guo L R, Wang H Y, Gu J Z, Yang Y, Kirillova M V, Kirillov A M. Coordination polymers constructed from an adaptable pyridine-dicarboxylic acid linker: Assembly, diversity of structures, and catalysis. *Inorg. Chem.*, **2022**,**61**(45):17951-17962